

The effect of exercise hypertrophy and disuse atrophy on muscle contractile properties: a mechanomyographic analysis

Christian Than¹ · Danijel Tosovic¹ · Laura Seidl¹ · J. Mark Brown¹

Received: 22 April 2016 / Accepted: 3 September 2016 / Published online: 10 September 2016
© Springer-Verlag Berlin Heidelberg 2016

Abstract

Purpose To determine whether mechanomyographic (MMG) determined contractile properties of the biceps brachii change during exercise-induced hypertrophy and subsequent disuse atrophy.

Methods Healthy subjects (mean \pm SD, 23.7 ± 2.6 years, BMI 21.8 ± 2.4 , $n = 19$) performed unilateral biceps curls (9 sets \times 12 repetitions, 5 sessions per week) for 8 weeks (hypertrophic phase) before ceasing exercise (atrophic phase) for the following 8 weeks (non-dominant limb; treatment, dominant limb; control). MMG measures of muscle contractile properties (contraction time; T_c , maximum displacement; D_{max} , contraction velocity; V_c), electromyographic (EMG) measures of muscle fatigue (median power frequency; MPF), strength measures (maximum voluntary contraction; MVC) and measures of muscle thickness (ultrasound) were obtained.

Results Two-way repeated measures ANOVA showed significant differences ($P < 0.05$) between treatment and control limbs. During the hypertrophic phase treatment MVC initially declined (weeks 1–3), due to fatigue (decline in MPF), followed by improvement against control during weeks 6–8. Between weeks 5 and 8 treatment, muscle thickness was greater than control, reflecting gross hypertrophy. MMG variables D_{max} (weeks 2, 7) and V_c (weeks 7, 8) declined. During the atrophic phase, MVC (weeks 9–12) and muscle thickness (weeks 9, 10) initially

remained high before declining to control levels, reflecting gross atrophy. MMG variables D_{max} (weeks 9, 14) and V_c (weeks 9, 14, 15) also declined during the atrophic phase. No change in T_c was found throughout the hypertrophic or atrophic phases.

Conclusions MMG detects changes in contractile properties during stages of exercise-induced hypertrophy and disuse atrophy suggesting its applicability as a clinical tool in musculoskeletal rehabilitation.

Keywords Mechanomyography (MMG) · Hypertrophy · Atrophy · Biceps brachii · Exercise

Abbreviations

ANOVA	Analysis of variance
BMI	Body mass index
CSA	Cross-sectional area
D_{max}	Maximal muscle belly displacement
DOMS	Delayed onset of muscle soreness
EMG	Electromyography
ES	Effect size
MMG	Mechanomyography
MPF	Median power frequency
MVC	Maximum voluntary contraction
PNS	Percutaneous neuromuscular stimulation
SD	Standard deviation
SEM	Standard error mean
T_c	Contraction time
V_c	Contraction velocity

Communicated by William J. Kraemer.

✉ Christian Than
christian.than@uqconnect.edu.au

¹ Department of Anatomy and Developmental Biology, School of Biomedical Sciences, The University of Queensland, St. Lucia 4072, Australia

Introduction

Patients often attend musculoskeletal clinics with atrophic muscles due to injury or disease. Often the aim of

rehabilitation is to hypertrophy wasted muscles to allow the patient to regain functional capacity. However, it remains difficult for clinicians to inexpensively detect and quantify hypertrophic changes in muscle throughout the rehabilitative process. Currently quantitative assessments of muscle bulk rely upon cost-intensive techniques such as magnetic resonance imaging (MRI), computed tomography (CT) or dual energy X-ray absorptiometry scan (DEXA) which are generally unavailable at most community-based facilities (Palus et al. 2014). Assessments of hypertrophy-related changes in muscle physiology (e.g., contractile properties) may prove to be an inexpensive solution to this problem. However, little evidence exists to indicate application of this in clinical settings, despite the documented differences in properties of hypertrophied and atrophied muscles (Bodine et al. 2001; Marcotte et al. 2015).

Skeletal muscle accounts for approximately 40 % of body mass and is highly adaptive due to changes in its utilisation (Brooks and Myburgh 2014). Increases in mechanical load, through increasing workload via rehabilitative exercises, will stimulate muscle hypertrophy while the removal of mechanical load, through inactivity or injury, will lead to muscle atrophy (Brooks and Myburgh 2014). Studies have shown that the onset of muscle atrophy occurs approximately 2 weeks after the onset of injury or immobilisation (de Boer et al. 2007; Abadi et al. 2009). In contrast, resistance training-induced muscle hypertrophy occurs predominantly during the first 10 weeks of training with significant change in muscle size occurring approximately 4 weeks following the initiation of hypertrophic exercise (Abe et al. 2000; Seynnes et al. 2007; DeFreitas et al. 2011; Ogasawara et al. 2012).

Recent evidence suggests that the mechanomyographic technique (MMG) may prove to be a cost-effective non-invasive method of detecting atrophic or hypertrophic changes in muscle contractile properties (Ibitoye et al. 2014). The MMG technique can characterise changes in the velocity of contraction (V_c), contraction time (T_c) and maximum muscle displacement (D_{max}) due to muscle fatigue and acute muscle injury (Madeleine et al. 2001; Gorelick and Brown 2007; Kassolik et al. 2009; Ibitoye et al. 2014), while it has been shown that MMG variables do not vary between opposite limb muscles in normal populations (Alvarez-Diaz et al. 2015).

The MMG technique functions through measuring the low-frequency lateral oscillation of a superficial muscle's belly following maximal involuntary percutaneous neuromuscular stimulation (PNS) (Sarlabous et al. 2013). MMG detects spatial and temporal changes in the size of the muscle belly during PNS-induced contractions as observed by the displacement of skin overlying the contracting muscle (Al-Mulla et al. 2011). Such measures are highly correlated to the development of tension within the belly and tendons

of the muscle itself (Orizio 1993; Orizio et al. 1999, 2000, 2003; McAndrew et al. 2006). MMG's inherent ability to quantify muscle function non-invasively potentially supports its use as a clinical tool within clinical settings (Kassolik et al. 2009; Ibitoye et al. 2014).

Therefore, the aim of this study was to determine whether MMG had utility in detecting changes in muscle contractile properties during an 8-week period of exercise-induced muscle hypertrophy and disuse induced atrophy, respectively, within the biceps brachii. It was hypothesised that measures of muscle contractibility (T_c , D_{max} , V_c) would improve while the muscle hypertrophied but would regress back to 'normal' during a period of muscle atrophy. Such a result would suggest the applicability of the MMG technique to provide quantitative data on muscle recovery during rehabilitation.

Methods

Subjects

Ethical clearance for this study was obtained from the University of Queensland Medical Research Ethics Committee (no. 2014001416) and informed consent was obtained from each subject. Subjects aged 18–30 years (mean \pm SD, 23.7 ± 2.6 years, BMI 21.8 ± 2.4 , $n = 19$) with no history of upper limb injuries were recruited for the study. Subjects were considered recreationally active, but not resistance trained (i.e., exercised $3 \times$ or more weekly via various sporting activities but had not performed resistance training for the biceps brachii). All results were analysed as percentage changes from baseline results obtained in week 0. Measurements were taken on allocated days to ensure approximate 7-day intervals between data collection points for each participant.

Mechanomyography (MMG)

Subjects were seated on a padded plinth with the elbow secured by large Velcro straps at 90° elbow flexion in a supinated position for laser sensor displacement mechanomyography measurements (Fig. 1). Baseline MMG readings in week 0 were taken for both the dominant and non-dominant biceps brachii with additional MMG readings taken at the end of each week throughout the 16-week study (Fig. 2). MMG measures of contractile properties are typically recorded from maximally stimulated muscles via a twitch stimulus (Tosovic et al. 2015). To maximally contract the biceps brachii, an initial stimulus of 30 mA was delivered with subsequent stimuli increasing by 10 mA whilst keeping a constant voltage (400 V) and duration (200 μ s) (Digitimer DS7AH) (Tosovic et al. 2015). A 30 s



Fig. 1 Demonstration of MMG protocol. After determining 50 % total length of the biceps brachii for MMG laser positioning, proximal and distal stimulator electrodes (TENS pads) were attached 25 mm apart. Upper limb was kept in 90° elbow flexion in a supinated position. Straps were secured around the arm and upper thoracic region to prevent excessive movement during stimulation. *MMG* mechanomyography

inter-stimuli interval was utilised to minimise fatigue. Stimuli of increasing current were delivered until a maximum muscle contraction was achieved as denoted by the largest maximum muscle displacement (D_{max}) value observed, without distortion of the sinusoidal MMG waveform (Tosovic et al. 2015).

To measure radial muscle belly displacement following PNS, a laser measurement device (class 2 laser; model LG10A65PU) was positioned perpendicular to the middle of the muscle belly of the biceps brachii, which was within the vicinity of the muscle’s approximate motor point (Moon et al. 2012). This position was midway between two PNS stimulatory electrodes (NeuroTrac TENS self-adhesive

electrodes; 30 mm diameter) which were positioned 25 mm either side of the muscle’s mid-length (50 mm inter-electrode distance). MMG contractile properties were calculated as mean values from five recordings of maximal MMG waveforms (Tosovic et al. 2015). The MMG waveforms were recorded in LabChart® software (ADInstruments), and analysis of maximum muscle displacement (D_{max-mm}), contraction time (T_{c-ms}) and contraction velocity ($V_{c-mm/ms}$) performed with the Peak Analysis module within LabChart®. It should be noted that V_c measurements are not absolute values although expressed as mm/ms due to incorporation of D_{max} (0–100 % of waveform) by T_c (10–90 % of waveform). A 9 Hz low-pass digital filter was applied in the recording of the waveforms (Tosovic et al. 2015).

Maximum voluntary contraction (MVC)

Maximum voluntary contraction force values (MVC-N) were obtained from isometric contractions of the biceps brachii in both upper limbs using a Sundoo SN Analogue Force Gauge (model number SN-500). Subjects lay supine whilst pulling on the force gauge at 90° elbow flexion.

Electromyography (EMG)

Median power frequency (MPF-Hz), as determined by electromyography (EMG), was recorded during the MVCs. Following skin preparation, a single pair of bipolar surface electrodes (inter-electrode distance of 4 mm) was placed longitudinally at 50 % of the total length of the biceps brachii (from origin to insertion) with a third ground electrode attached to the anterior surface of the clavicle. All three electrodes were connected to an ADInstruments Powerlab

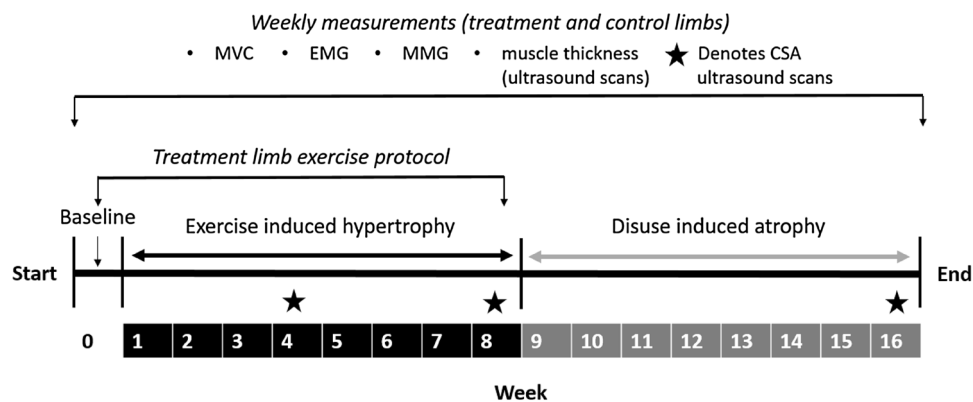


Fig. 2 Study timeline. After obtaining baseline results in week 0 for the weekly measurements of MVC, EMG, MMG and muscle thickness, the treatment (non-dominant) limb underwent exercise-induced hypertrophy from weeks 0–8 (black colour filled square). Exercise consisted of a dumbbell loaded at 70, 50 or 30 % of MVC (12 repetitions for 9 sets with 90 s inter-set rest intervals) performed 5x weekly.

Exercise for the treatment limb ceased from weeks 9–16 to induce atrophy (gray colour filled square). The control (dominant) limb did not perform any exercise throughout the study. CSA ultrasound scans were conducted in weeks 4, 8 and 16. CSA cross-sectional area, EMG electromyography, MMG mechanomyography, MVC maximum voluntary contraction

system via a dual bioamp (sample rate 1 kb/s; range 10 V; high pass digital filter 20 Hz). Analysis was conducted in LabChart 7 Pro™.

Ultrasound scans

After baseline MMG readings were obtained, baseline muscle thickness ultrasound recordings were taken, with additional readings once again taken at the end of each week throughout the 16 weeks (Fig. 2). Subjects were seated with arms in a neutral position around the elbow joint as advised by a qualified ultra-sonographer. The subjects' dominant and non-dominant biceps brachii were scanned using a 7.5 MHz linear transducer probe (Mindray DP-50). The scans were taken in B-mode with ultrasound machine settings (gain, depth and frequency) adjusted to optimise image quality for individuals. Measurements were taken at 50 % total length of the biceps brachii.

During weeks 4, 8 and 16, additional cross-sectional area (CSA) ultrasounds for both upper limbs were obtained by a qualified ultra-sonographer at the Centre of Advanced Imaging at The University of Queensland (Fig. 2). Using a standard 4–9 MHz linear transducer operating on 9 MHz (S3000 Siemens/Acuson system), images were obtained in B-mode. Participants were seated in an upright position with arms in a neutral position around the elbow joint. CSA images were obtained via lateral acquisition at 50 % width of the bicep brachii. Muscle thickness and CSA from ultrasound images were determined using ImageJ (version 1.48; National Institutes of Health, Bethesda, MD). Week 4 thickness ultrasounds are missing due to conflicting scheduling with CSA ultrasounds.

Exercise protocol

After baseline recordings, subjects underwent a strength training regime to induce muscle hypertrophy in the non-dominant limb (treatment) from week 0 (Fig. 2). The protocol consisted of the non-dominant upper limb performing unilateral bicep curls (elbow flexion with a supinated forearm) with a dumbbell loaded to 70, 50 or 30 % of that week's MVC recording. Participants performed the exercise at the 70 % loading before progressively lowering the lifting weight to 50 %, and then finally 30 %, loading due to failure to maintain correct form with the previous dumbbell weight. A total of 9 sets of 12 bicep curl repetitions per set were performed with a 90 s rest interval assigned between each set. This loading strategy has been hypothesised as the ideal combination of mechanical tension and metabolic stress to maximise a hypertrophic response (Schonenfeld 2010).

The exercise protocol was performed five times weekly for a total of 8 weeks (weeks 0–8), with sessions

approximately 24 h apart. Kraemer et al. (2002) have stated that training frequency should be 2–3 times weekly for novice training and 4–5 times weekly for advanced training. As muscle is adaptable, participants would eventually progress to the advanced fitness level during the hypertrophy phase (Brooks and Myburgh 2014). The precise point at which this occurs would be different for each participant due to factors such as amino acid availability and hormone presence (Tipton and Wolfe 2001). Thus, in order to standardise the protocol, a five times weekly training regime was chosen from the beginning of the program. As all participants were novice lifters at the start of the protocol, the 70, 50 and 30 % MVC progression was employed. This in turn would allow individuals to perform the exercise for each session as their body would allow to offset overtraining and fatigue effects.

At the end of each week, biceps brachii MVC values were once again obtained from both the dominant and non-dominant upper limbs. After week eight recordings, subjects ceased the exercise regime to initiate disuse muscle atrophy (Fig. 2). The dominant biceps brachii of each subject served as the control for the study throughout the hypertrophic and atrophic periods of the study. Subjects were required to refrain from active exercise involving the biceps brachii, other than daily activities, throughout the 16 weeks.

Statistical analysis

Data points identified as outliers, in accordance with accepted statistical outlier detection, were removed before analysis (Rousseeuw and Hubert 2011). Out of 646 total values for one parameter, seven values were removed from treatment limb data whilst 33 values were removed from control limb data.

Repeated measures two-way ANOVAs were conducted in Graph Pad Prism 6 (limb group x week) to determine whether muscle hypertrophy and atrophy had a significant effect on MMG-derived contractile properties. If significance was obtained ($P < 0.05$), protected fishers LSD post hoc was used to identify location of significance. Cohen effect sizes (ES) were calculated to determine the magnitude of significance with Cohen (1988) defining ES descriptors as trivial (<0.2), small (>0.2 – <0.5), medium (>0.5 – <0.8) and large (>0.8). Data are represented as means and standard errors of the means (\pm). Variables analysed were MVC, MPF, CSA, muscle thickness, contraction time (T_c), maximal muscle belly displacement (D_{max}) and contraction velocity (V_c). Reliability of MMG-derived contractile properties has previously been determined (Krizaj et al. 2008; Tous-Fajardo et al. 2010; Ditroilo et al. 2013).

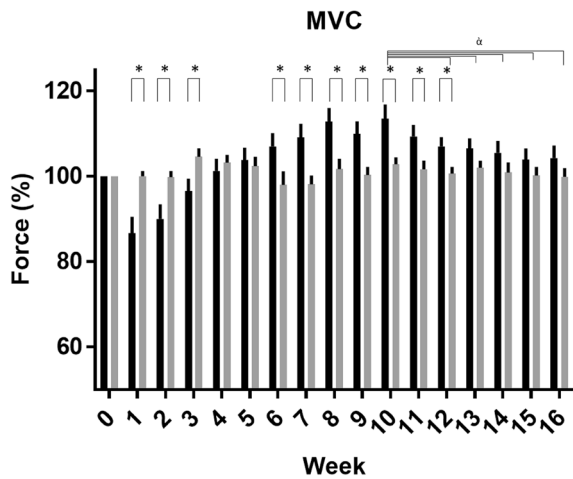


Fig. 3 MVC. Mean (\pm SEM) treatment (black colour filled square) and control (gray colour filled square) limb MVC values each week. Single asterisk indicates significant ($P < 0.05$) difference between limbs for each week. Δ indicates significant ($P < 0.05$) difference between treatment alone. Changes are as a percentage from week 0 baseline. MVC maximum voluntary contraction, SEM standard error of mean

Results

MVC and MPF

During weeks 1–3 of the hypertrophic phase, MVCs from the treatment limb declined against the control limb ($P < 0.05$) (Cohen ES of 1.21, 0.97 and 0.86) before then overtaking the control limb during weeks 6–8 ($P < 0.05$) (Cohen ES of 0.74, 1.09, and 1.05) (Fig. 3). During the atrophic phase, treatment limb MVC values initially remained higher than control (weeks 9–12, Cohen ES of 1.05, 1.10, 0.86 and 0.97) ($P < 0.05$) before declining to the control values (Fig. 3). For the treatment limb, the MVC in week 10 was significantly larger than in weeks 12–16 ($P < 0.05$) (Cohen ES of 0.62, 0.65, 0.69, 0.86 and 0.77).

The MPF values suggested that during the hypertrophic phase the treatment limb was experiencing significantly ($P < 0.05$) greater muscle fatigue than the control limb (weeks 1–6)—at a time when the treatment limb’s MVC values had declined. No differences in MPF were seen between treatment and control limbs during the atrophic phase of the study (Fig. 4). Cohen ES for weeks 1–6 were 0.74, 1.06, 1.19, 1.08, 0.66 and 0.76.

Muscle cross-sectional area

The ultrasound images showed the treatment limb to have a significantly ($P < 0.05$) larger CSA than control by the end of the hypertrophic phase (week 8), with a Cohen ES of 0.59, which had dissipated by the end of the atrophic phase

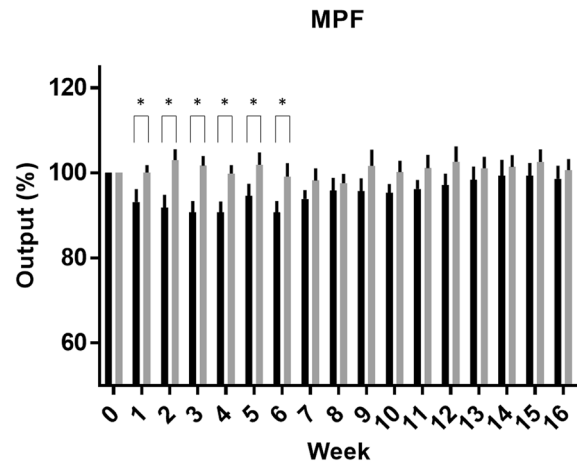


Fig. 4 MPF of EMG. Mean (\pm SEM) treatment (black colour filled square) and control (gray colour filled square) limb MPF values each week. Single asterisk indicates significant ($P < 0.05$) difference between limbs for each week. Changes are as a percentage from week 0 baseline. EMG electromyography, MPF median power frequency, SEM standard error of mean

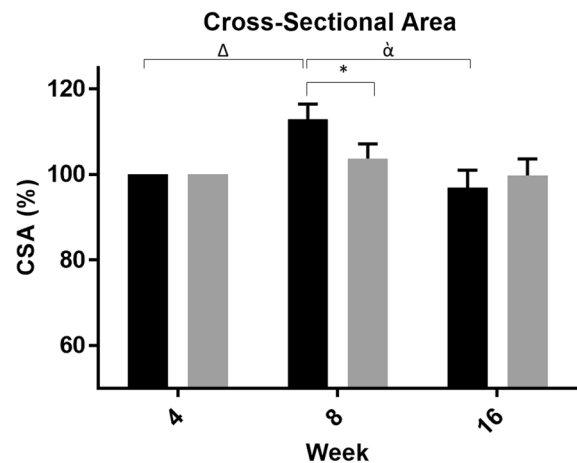


Fig. 5 CSA ultrasound. Mean (\pm SEM) treatment (black colour filled square) and control (gray colour filled square) limb CSA ultrasounds values at the end of week 4 (baseline), week 8 (hypertrophy end) and week 16 (atrophy end). Single asterisk indicates significant ($P < 0.05$) difference between limbs for each week. Δ indicates significant ($P < 0.05$) difference between treatment alone. Triangle indicates significant difference ($P < 0.05$) between treatment baseline. Changes are as a percentage from week 4 baseline. Note: due to ethical acceptance delays with the Centre of Advanced Imaging, week 0 CSA ultrasounds are substituted with week 4 CSA ultrasounds. CSA cross-sectional area, SEM standard error of mean

in week 16 (Fig. 5). Muscle thickness demonstrated that the treatment limb was thicker than control during weeks 5–8 of the hypertrophic phase ($P < 0.05$) with Cohen ES of 0.94, 0.57, 0.62 and 0.82. This was also demonstrated during the initial weeks of the atrophic phase (Weeks 9–10, Cohen ES of 0.49 and 0.51) ($P < 0.05$) (Fig. 6).

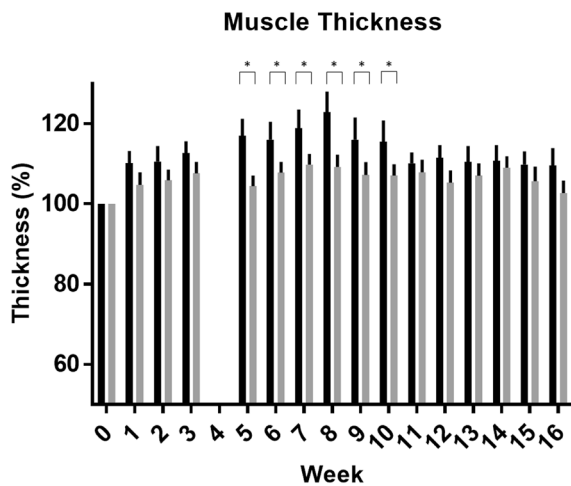


Fig. 6 Muscle thickness from ultrasound scans. Mean (\pm SEM) treatment (black colour filled square) and control (gray colour filled square) limb thickness ultrasounds values. Single asterisk indicates significant ($P < 0.05$) difference between limbs for each week. Changes are as a percentage from week 0 baseline. Note: Week 4 thickness ultrasounds are missing due to conflicting scheduling with CSA ultrasounds. CSA cross-sectional area, SEM standard error of mean

Contraction time (T_c)

No significant change in muscle contraction time (T_c) was noted in either limb throughout the study (Fig. 7). The T_c of the treatment biceps brachii during baseline (week 0), end of hypertrophy (week 8) and end of atrophy (week 16) was 53.44 ms, 51.93 ms and 51.86 ms, respectively, whilst control T_c values were 52.19 ms, 49.72 ms and 51.07 ms, respectively.

Maximal muscle belly displacement (D_{max})

D_{max} of the treatment limb was significantly lower than the control limb during weeks 2 and 7 ($P < 0.05$) of the hypertrophic phase (Cohen ES of 0.47 and 0.59), week 9 of the initial atrophic phase and then later in the atrophic phase at week 14 ($P < 0.05$) (Cohen ES of 0.42 and 0.86) (Fig. 8).

Contraction velocity (V_c)

V_c of the treatment limb was significantly slower, against control, late in the hypertrophic phase (weeks 7–8 with Cohen ES of 0.60 and 0.54), the early atrophic phase (week 9, Cohen ES of 0.46) and then later in the atrophic phase (weeks 14–15, Cohen ES of 0.87 and 0.75) ($P < 0.05$) (Fig. 9).

Discussion

The aim of the study was to clarify the utility of the MMG technique to quantify changes in muscle contractile

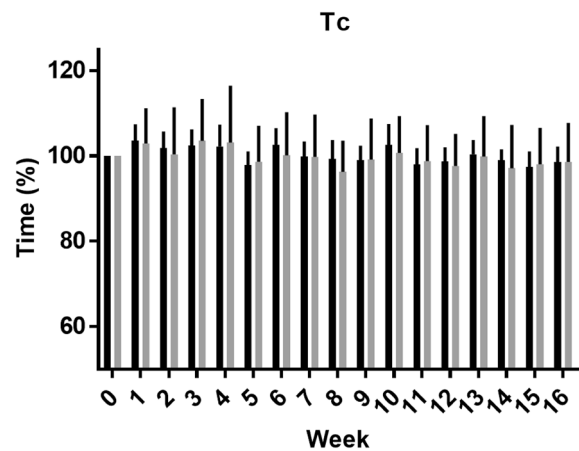


Fig. 7 T_c . Mean (\pm SEM) treatment (black colour filled square) and control (gray colour filled square) limb T_c values each week. No significance was obtained within or between limbs. Changes are as a percentage from week 0 baseline. T_c contraction time, SEM standard error of mean

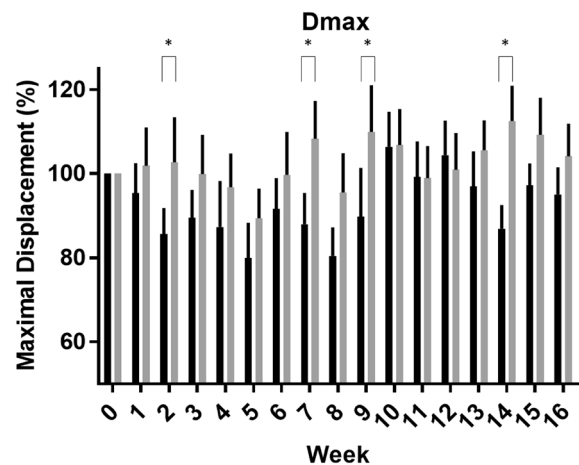


Fig. 8 D_{max} . Mean (\pm SEM) treatment (black colour filled square) and control (gray colour filled square) limb D_{max} values each week. Single asterisk indicates significant ($P < 0.05$) difference between limbs for each week. Changes are as a percentage from week 0 baseline. D_{max} maximal muscle displacement, SEM standard error of mean

properties related to muscle hypertrophy and atrophy—two muscular conditions common to clinical musculoskeletal rehabilitation. The current study is believed to be the first to employ MMG to determine changes in muscle contractile properties during a period of exercise-induced hypertrophy followed by a period of disuse atrophy.

Strength measures (MVC and MPF)

MVC for weeks 1–3 of the hypertrophic phase was found to be significantly lower ($P < 0.05$) in the treatment limb

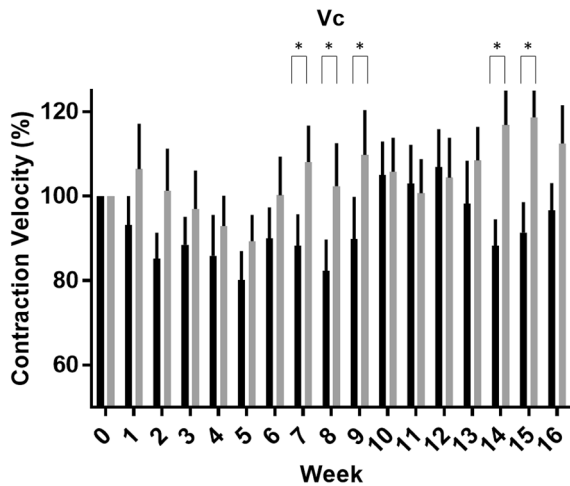


Fig. 9 V_c . Mean (\pm SEM) treatment (black colour filled square) and control (gray colour filled square) limb V_c values each week. Single asterisk indicates significant ($P < 0.05$) difference between limbs for each week. Changes are as a percentage from week 0 baseline. V_c contraction velocity, SEM standard error of mean

than the control limb (Fig. 3). The decline in MVC for the treatment limb is theorised to be attributed to injury/fatigue from the intensive exercise protocol (Cheung et al. 2003). Exercise involving eccentric contractions has been documented to cause micro-injury within the muscle (Mizumura and Taguchi 2015). This structural damage to muscle and connective tissue leads to delayed onset of muscle soreness (DOMS), which may result in alterations to muscle function and joint mechanics (Cheung et al. 2003; Wiewelhove et al. 2016). Studies have documented significant reductions in strength and power parameters during DOMS, which subsides and eventually disappears by 3–10 days post-exercise (Wheeler and Jacobson 2013). The exercise protocol employed by this study had participants performing strenuous eccentric-based contractions 5 days a week to ensure eventual hypertrophy. As such, participants are speculated to have been in an initial constant state of DOMS during the onset of the hypertrophy phase, providing possible explanation for the reduced treatment MVC results for weeks 1–3.

However, skeletal muscle rapidly adapts to its mechanical environment due to its plastic nature (Goldberg 1968; Marcotte et al. 2015). Increased load across a muscle, such as from the resistance exercise protocol conducted in the study, results in a compensatory increase in muscle size and strength (Marcotte et al. 2015). This hypertrophy occurs largely from the growth of existing cells (hypertrophy) rather than an increase in cell number (hyperplasia) (Goodman et al. 2011; Marcotte et al. 2015). Additionally, skeletal muscle fibres adapt through expression of specific contractile proteins, such as myosin heavy chain isoforms,

with upregulation in the activity and content of mitochondria to increase oxidative capacity (Holloszy and Booth 1976; Rockl et al. 2007). These adaptations in response to exercise support weeks 4–5 of the study, during which no significant differences were found between limbs, before treatment achieved higher MVCs than control ($P < 0.05$) in weeks 6–8 (Fig. 3). The relationships between muscle size, or CSA, and measures of performance are underpinned by the capability of muscle to produce force, with greater muscle CSA corresponding to greater force production (Vigotsky et al. 2015). As such, the ongoing increase in size of the treatment limb from the exercise protocol led to the eventual increase in strength measures, as seen in weeks 6–8 of the hypertrophic phase.

This perceived eventual adaptation of muscles to exercise is further supported by the MPF results from the EMG waveforms. The treatment limb demonstrated fatigue against the control limb for weeks 1–6 ($P < 0.05$) due to exercise (Fig. 4). However, compensatory adaptation enables muscles to more efficiently use substrates for ATP production, providing the treatment limb fatigue resistance which was seen from week 7 onwards for the MPF results (Rockl et al. 2007).

During the atrophic phase of the study, the treatment limb had a higher initial MVC than control during weeks 9–12 ($P < 0.05$) (Fig. 3). Maintenance of muscle mass is controlled by a balance between protein synthesis and protein degradation pathways, with shifts towards protein degradation during atrophy (Bodine et al. 2001). Atrophy occurs as an adaptive response to de-loading, with Dirks et al. (2015) finding 1 week of strict bed rest enough to cause significant reduction in muscle mass. In terms of strength measures (MVC), the study showed a decline in MVC from week 13 (Fig. 3) simultaneously with declines in muscle thickness (Fig. 6), suggesting atrophy from this point onwards.

In humans, common disuse models include bed rest or plaster casts (Narici et al. 2016). In these studies, a significant decrease in efferent motor outflow (neural drive) to target muscles occurs due to inactivity of spinal motor neurons (Aagaard et al. 2002; Gondin et al. 2004). Gibson et al. (1988) found that low-voltage percutaneous electrical stimulation, akin to neural drive, reduces atrophy via prevention of muscle protein synthesis decreases that accompany immobilisation. The present study permitted everyday use of the treatment limb throughout the atrophic phase which is more reflective of real life situations employing simple disuse atrophy after mechanical loading. Therefore, the neural drive received by the treatment limb from everyday use could have in turn slowed atrophy of the muscle (Gibson et al. 1988). This in turn could explain the delay in atrophy for the treatment limb to return to control limb MVC values.

Despite this, weeks 13–16 of the atrophic phase saw no significant difference between limbs, indicating disuse atrophy of the treatment limb back to the control level. Additionally, week 10 treatment was found to be significantly higher than itself in weeks 12–16 ($P < 0.05$). It, therefore, appears as if week 10 was the final measurement before treatment began its decline in MVC, possibly attributed to initial declines in neuromuscular adaptation from cessation of resistance training (Deschenes et al. 2002), before declining from week 13 onwards as supported by muscle thickness scans (Fig. 6).

Muscle size (CSA and muscle thickness)

The MVC results were consistent with both the CSA (Fig. 5) and muscle thickness (Fig. 6) measures in which treatment limb was significantly larger than control by week 8 ($P < 0.05$) but not different again by week 16. These results support the contention that the treatment limb hypertrophied and atrophied, respectively, throughout the study.

The muscle thickness values demonstrated that the treatment limb was larger than control in weeks 5–8 of the hypertrophic phase. The literature indicates that 4 weeks of resistance training should be enough to induce significant muscle hypertrophy (Abe et al. 2000; Seynnes et al. 2007; DeFreitas et al. 2011; Ogasawara et al. 2012). Although the week 4 thickness results were omitted, the week 5 thickness measures support the results of previous literature. Additionally, the week 10 muscle thickness measure was the final measurement in which treatment was significantly larger than control ($P < 0.05$). Week 11 onwards demonstrated no significant difference between limbs, indicating atrophy of the treatment limb following 2 weeks of ceasing resistance training. This was consistent with previous literature regarding the onset timeframe of atrophy (de Boer et al. 2007; Abadi et al. 2009).

Contractile properties (MMG)

T_c and V_c reflect time-domain activation of motor units during both isometric and dynamic muscle actions (Beck et al. 2004). In contrast, the amplitude-domain D_{max} relates to the intensity of motor unit recruitment with a linear relationship between D_{max} and the work load of the contracting muscle (Beck et al. 2004; Al-Mulla et al. 2011).

As such, these MMG parameters will vary when skeletal muscle undergoes morphological changes and remodeling during phases of growth and wasting (Pisot et al. 2008; DeFreitas et al. 2012). D_{max} was significantly lower for the treatment limb against control in weeks 2 and 7 of the hypertrophic phase (Fig. 8). During hypertrophy, contractile structures enlarge (increase of sarcomeres and myofibrils added

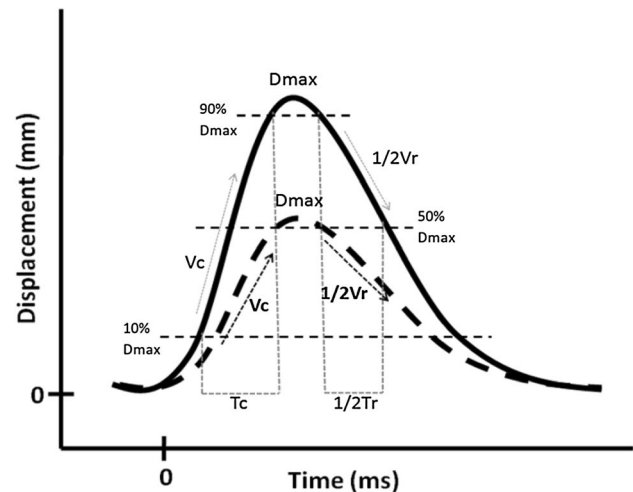


Fig. 10 Idealised MMG waveform. Demonstrates changes in the waveform from muscle remodelling during phases of hypertrophy and atrophy; reflective of the results observed in this study. *Filled line* indicates normal MMG waveform of healthy muscle in a stable state. *Broken line* indicates a weakened MMG waveform seen during muscle remodelling through hypertrophy and atrophy. Waveform shows a decrease in D_{max} , but no change in T_c , thus decreasing the slope (velocity) of contraction. The descending portion of the waveform correlates to relaxation time of the muscle, which was not relevant to the findings of the current study. D_{max} (mm) maximal muscle displacement, T_c (ms) contraction time (between 10–90 % of D_{max}), $1/2Tr$ (ms) half-relaxation time (between 90 and 50 % of D_{max}), V_c (mm/ms) contraction velocity (D_{max} divided by T_c), $1/2Vr$ half-relaxation velocity (D_{max} divided by $1/2Tr$)

in parallel) and the extracellular matrix expands (Tesch and Larsson 1982; Vierck et al. 2000; Paul and Rosenthal 2002; Schoenfeld 2010). These intrinsic changes within muscle in turn lead to altered contractile properties and motor unit recruitment patterns (Blaauw et al. 2013). In weeks 2 and 7 of the hypertrophic phase, treatment limb D_{max} was significantly lower than control ($P < 0.05$). While week 2 significance can be attributed to fatigue of the treatment limb from DOMS (Cheung et al. 2003), week 7 suggests intrinsic changes in the recruitment pattern of motor neurons to cause maximal muscle belly displacement. This change in neural control was reflected in the amplitude of the MMG waveform as a significantly diminished curve height (Fig. 10).

Changes in contractile properties during disuse caused significantly diminished treatment MMG waveforms in weeks 9 and 14 ($P < 0.05$) of the atrophy phase (Fig. 8). Deschenes et al. (2002) have shown that diminishment in muscle function is mainly attributed to neural activation decline 2 weeks post-cessation of resistance training. The significant difference in D_{max} between limbs in week 9 on the experiment was contrary with the MVC (Fig. 3) and thickness scans (Fig. 6) that indicated treatment hypertrophy. Thus, decline in D_{max} during week 9 may in turn be indicative of continuing remodelling of contractile properties from

the hypertrophy phase rather than muscle atrophy. However, the week 14 result paralleled MVC and thickness scans to suggest changes to not only neural recruitment patterns as Deschenes et al. (2002) described, but also atrophy.

Atrophy of a muscle can lead to altered contractile properties and recruitment patterns (Blaauw et al. 2013) with Narici and Cerretelli (1998) finding disuse atrophy to decrease muscle fascicle length and pennation angle, to indicate loss of sarcomeres in series and in parallel. The simultaneous decreases in D_{\max} , MVC and ultrasound treatment found in week 14 are, thus, in line with the literature to support significant atrophy and changes to neurological motor recruitment of the treatment limb in week 14.

T_c of the treatment limb, which is the time taken to complete physiological actin/myosin cross bridging (MacIntosh et al. 2012), did not change significantly throughout the study (Fig. 7).

However, the velocity of contraction (V_c), which physiologically corresponds to the speed/efficiency of actin–myosin cross-bridge formation with respect to motor unit recruitment (MacIntosh et al. 2012; Tosovic et al. 2016), did achieve significance between limbs in weeks 7 and 8 of hypertrophy (Fig. 9). As stated before, MMG parameters will change when skeletal muscle undergoes morphological changes and remodelling. This was evident in treatment limb V_c , which is reflective in the ascending slope of contraction in an MMG waveform (Fig. 10). During weeks 7 and 8 of hypertrophy, the treatment limb was found to have a slower V_c than control ($P < 0.05$), suggesting pronounced modification of muscle architecture from hypertrophy. This slowed treatment V_c was additionally found in weeks 9, 14 and 15 ($P < 0.05$) of the atrophy phase, indicative of inherent changes within the muscle during the disuse phase.

Due to the structure of the MMG waveform, physiological muscle parameters are linked together and change accordingly. Thus, when the amplitude of the waveform diminishes (D_{\max}), the ascending slope (V_c) of the MMG waveform will diminish synchronously to maintain a constant contraction time (T_c) (Fig. 10). This was observed in the study in which D_{\max} and V_c of the treatment limb changed generally parallel to each other, despite a stable T_c throughout the hypertrophic and atrophic phases. Physiologically, this demonstrates that alterations in neurological recruitment are somewhat coordinated with the velocity of actin–myosin cross-bridge formation to maintain a stable time for the power stroke of contraction. The exact mechanisms on which this occurs remain to be elucidated.

It should be noted that unilateral motor unit activity has been documented to affect the homologous contralateral limb in a phenomenon known as cross education (Zhou 2000). There is a, thus, limitation in using the dominant limb as a control for the study as neural adaptations in the treatment limb could have carried over to the control

limb to affect the results (Zhou 2000). Nevertheless, MMG appeared to be able to identify changes in contractile properties throughout the study.

Conclusion

This investigation utilised mechanomyography (MMG) to non-invasively quantify changes in biceps brachii contractile properties following 8 weeks of exercise-induced hypertrophy (rehabilitation) and a further 8 weeks of disuse induced atrophy (injury). The MVC and ultrasound results suggest that the treatment limb experienced hypertrophy and subsequent atrophy during these two periods. The results suggest that MMG was able to detect changes in muscle contractile properties only within the treatment limb during the hypertrophic and atrophic phases of the study. Therefore, the MMG technique may have utility in the clinical environment as an inexpensive and non-invasive assessment aid of injured patients, allowing quantification of their return to full function following rehabilitation.

Acknowledgments The authors wish to thank The University of Queensland for their postgraduate support and each of the participants for their commitment to completing this study. The authors would also like to thank Ms. Gail Durbridge from the Centre of Advanced Imaging, located at the St. Lucia campus of the University of Queensland, for performing the CSA ultrasound scans. The authors also acknowledge Dr. Carl Stephan for the supply of ultrasound gel used for thickness scans.

Compliance with ethical standards

Conflict of interest The authors declare that they have no conflict of interest.

References

- Aagaard P, Simonsen EB, Andersen JL, Magnusson P, Dyhre-POULSEN P (2002) Increased rate of force development and neural drive of human skeletal muscle following resistance training. *J Appl Physiol* (1985) 93:1318–1326
- Abadi A, Glover EI, Isfort RJ, Raha S, Safdar A, Yasuda N, Kaczor JJ, Melov S, Hubbard A, Qu X, Phillips SM, Tarnopolsky M (2009) Limb immobilization induces a coordinate down-regulation of mitochondrial and other metabolic pathways in men and women. *PLoS One* 4:e6518
- Abe T, Dehoyos DV, Pollock ML, Garzarella L (2000) Time course for strength and muscle thickness changes following upper and lower body resistance training in men and women. *Eur J Appl Physiol* 81:174–180
- Al-Mulla MR, Sepulveda F, Colley M (2011) A review of non-invasive techniques to detect and predict localised muscle fatigue. *Sensors (Basel)* 11:3545–3594
- Alvarez-Diaz P, Alentorn-Geli E, Ramon S, Marin M, Steinbacher G, Rius M, Seijas R, Ballester J, Cugat R (2015) Effects of anterior cruciate ligament reconstruction on neuromuscular tensiomyographic characteristics of the lower extremity in competitive male soccer players. *Knee Surg Sports Traumatol Arthrosc* 23:3407–3413

- Beck TW, Housh TJ, Johnson GO, Weir JP, Cramer JT, Coburn JW, Malek MH (2004) Mechanomyographic amplitude and mean power frequency versus torque relationships during isokinetic and isometric muscle actions of the biceps brachii. *J Electromyogr Kinesiol* 14:555–564
- Blaauw B, Schiaffino S, Reggiani C (2013) Mechanisms modulating skeletal muscle phenotype. *Compr Physiol* 3:1645–1687
- Bodine SC, Latres E, Baumhueter S, Lai VK, Nunez L, Clarke BA, Poueymirou WT, Panaro FJ, Na E, Dharmarajan K, Pan ZQ, Valenzuela DM, Dechiara TM, Stitt TN, Yancopoulos GD, Glass DJ (2001) Identification of ubiquitin ligases required for skeletal muscle atrophy. *Science* 294:1704–1708
- Brooks NE, Myburgh KH (2014) Skeletal muscle wasting with disuse atrophy is multi-dimensional: the response and interaction of myonuclei, satellite cells and signaling pathways. *Front Physiol* 5:99
- Cheung K, Hume P, Maxwell L (2003) Delayed onset muscle soreness: treatment strategies and performance factors. *Sport Med* 33:145–164
- Cohen J (1988) Statistical power analysis for the behavioral sciences, 2nd edn. Lawrence Erlbaum Associates, Hillsdale, NJ
- de Boer MD, Maganaris CN, Seynnes OR, Rennie MJ, Narici MV (2007) Time course of muscular, neural and tendinous adaptations to 23 day unilateral lower-limb suspension in young men. *J Physiol* 583:1079–1091
- Defreitas JM, Beck TW, Stock MS, Dillon MA, Kasishke PR (2011) An examination of the time course of training-induced skeletal muscle hypertrophy. *Eur J Appl Physiol* 111:2785–2790
- Defreitas JM, Beck TW, Stock MS (2012) Effects of strength training on mechanomyographic amplitude. *Physiol Meas* 33:1353–1361
- Deschenes MR, Giles JA, McCoy RW, Volek JS, Gomez AL, Kraemer WJ (2002) Neural factors account for strength decrements observed after short-term muscle unloading. *Am J Physiol Regul Integr Comp Physiol* 282:R578–R583
- Dirks M, Wall B, Goossens G, Van de Valk B, Van Loon L (2015) One week of bed-rest substantially reduces muscle mass and induces insulin resistance in healthy young males. *FASEB J* 29
- Ditroilo M, Smith IJ, Fairweather MM, Hunter AM (2013) Long-term stability of tensiomyography measured under different muscle conditions. *J Electromyogr Kinesiol* 23:558–563
- Gibson JN, Smith K, Rennie MJ (1988) Prevention of disuse muscle atrophy by means of electrical stimulation: maintenance of protein synthesis. *Lancet* 2:767–770
- Goldberg AL (1968) Protein synthesis during work-induced growth of skeletal muscle. *J Cell Biol* 36:653–658
- Gondin J, Guette M, Maffiuletti NA, Martin A (2004) Neural activation of the triceps surae is impaired following 2 weeks of immobilization. *Eur J Appl Physiol* 93:359–365
- Goodman CA, Frey JW, Mabrey DM, Jacobs BL, Lincoln HC, You JS, Hornberger TA (2011) The role of skeletal muscle mTOR in the regulation of mechanical load-induced growth. *J Physiol* 589:5485–5501
- Gorelick ML, Brown JM (2007) Mechanomyographic assessment of contractile properties within seven segments of the human deltoid muscle. *Eur J Appl Physiol* 100:35–44
- Holloszy JO, Booth FW (1976) Biochemical adaptations to endurance exercise in muscle. *Annu Rev Physiol* 38:273–291
- Ibitoye MO, Hamzaid NA, Zuniga JM, Abdul Wahab AK (2014) Mechanomyography and muscle function assessment: a review of current state and prospects. *Clin Biomech (Bristol, Avon)* 29:691–704
- Kassolik K, Jaskolska A, Kisiel-Sajewicz K, Marusiak J, Kawczynski A, Jaskolski A (2009) Tensegrity principle in massage demonstrated by electro- and mechanomyography. *J Bodyw Mov Ther* 13:164–170
- Kraemer WJ, Adams K, Cafarelli E, Dudley GA, Dooly C, Feigenbaum MS, Fleck SJ, Franklin B, Fry AC, Hoffman JR, Newton RU, Potteiger J, Stone MH, Ratamess NA, Triplett-McBride T (2002) American College of Sports Medicine position stand. Progression models in resistance training for healthy adults. *Med Sci Sport Exerc* 34:364–380
- Krizaj D, Simunic B, Zagar T (2008) Short-term repeatability of parameters extracted from radial displacement of muscle belly. *J Electromyogr Kinesiol* 18:645–651
- Macintosh BR, Holash RJ, Renaud JM (2012) Skeletal muscle fatigue—regulation of excitation-contraction coupling to avoid metabolic catastrophe. *J Cell Sci* 125:2105–2114
- Madeleine P, Bajaj P, Sogaard K, Arendt-Nielsen L (2001) Mechanomyography and electromyography force relationships during concentric, isometric and eccentric contractions. *J Electromyogr Kinesiol* 11:113–121
- Marcotte GR, West DW, Baar K (2015) The molecular basis for load-induced skeletal muscle hypertrophy. *Calcif Tissue Int* 96:196–210
- McAndrew D, Gorelick M, Brown JMM (2006) Muscles within muscles: a mechanomyographic analysis of muscle segment contractile properties within human gluteus maximus. *J Musculoskelet Res* 10:23–35
- Moon JY, Hwang TS, Sim SJ, Chun SI, Kim M (2012) Surface mapping of motor points in biceps brachii muscle. *Ann Rehabil Med* 36:187–196
- Narici M, Cerretelli P (1998) Changes in human muscle architecture in disuse-atrophy evaluated by ultrasound imaging. *J Gravit Physiol* 5:P73–P74
- Narici M, Franchi M, Maganaris C (2016) Muscle structural assembly and functional consequences. *J Exp Biol* 219:276–284
- Ogasawara R, Thiebaud RS, Loenneke JP, Loftin M, Abe T (2012) Time course for arm and chest muscle thickness changes following bench press training. *Interv Med Appl Sci* 4:217–220
- Orizio C (1993) Muscle sound: bases for the introduction of a mechanomyographic signal in muscle studies. *Crit Rev Biomed Eng* 21:201–243
- Orizio C, Diemont B, Esposito F, Alfonsi E, Parrinello G, Moglia A, Veicsteinas A (1999) Surface mechanomyogram reflects the changes in the mechanical properties of muscle at fatigue. *Eur J Appl Physiol Occup Physiol* 80:276–284
- Orizio C, Baratta RV, Zhou BH, Solomonow M, Veicsteinas A (2000) Force and surface mechanomyogram frequency responses in cat gastrocnemius. *J Biomech* 33:427–433
- Orizio C, Gobbo M, Veicsteinas A, Baratta RV, Zhou BH, Solomonow M (2003) Transients of the force and surface mechanomyogram during cat gastrocnemius tetanic stimulation. *Eur J Appl Physiol* 88:601–606
- Palus S, von Haehling S, Springer J (2014) Muscle wasting: an overview of recent developments in basic research. *J Cachex Sarcopenia Muscle* 5:193–198
- Paul AC, Rosenthal N (2002) Different modes of hypertrophy in skeletal muscle fibers. *J Cell Biol* 156:751–760
- Pisot R, Narici MV, Simunic B, de Boer M, Seynnes O, Jurdana M, Biolo G, Mekjavic IB (2008) Whole muscle contractile parameters and thickness loss during 35-day bed rest. *Eur J Appl Physiol* 104:409–414
- Rockl KS, Hirshman MF, Brandauer J, Fujii N, Witters LA, Goodyear LJ (2007) Skeletal muscle adaptation to exercise training: AMP-activated protein kinase mediates muscle fiber type shift. *Diabetes* 56:2062–2069
- Rousseeuw PJ, Hubert M (2011) Robust statistics for outlier detection. *Wiley Interdiscip Rev Data Min Knowl Discov* 1:73–79
- Sarlabous L, Torres A, Fiz JA, Morera J, Jane R (2013) Index for estimation of muscle force from mechanomyography based on the Lempel-Ziv algorithm. *J Electromyogr Kinesiol* 23:548–557

- Schoenfeld BJ (2010) The mechanisms of muscle hypertrophy and their application to resistance training. *J Strength Cond Res* 24:2857–2872
- Seynnes OR, DE Boer M, Narici MV (2007) Early skeletal muscle hypertrophy and architectural changes in response to high-intensity resistance training. *J Appl Physiol* (1985) 102:368–373
- Mizumura K, Taguchi, T (2015) Delayed onset muscle soreness: involvement of neurotrophic factors. *J Physiol Sci*
- Tesch PA, Larsson L (1982) Muscle hypertrophy in bodybuilders. *Eur J Appl Physiol Occup Physiol* 49:301–306
- Tipton KD, Wolfe RR (2001) Exercise, protein metabolism, and muscle growth. *Int J Sport Nutr Exerc Metab* 11:109–132
- Tosovic D, Seidl L, Ghebremedhin E, Brown MJ (2015) Determining minimal stimulus intensity for mechanomyographic analysis. *J Electromyogr Kinesiol* 25:749–753
- Tosovic D, Than C, Brown JM (2016) The effects of accumulated muscle fatigue on the mechanomyographic waveform: implications for injury prediction. *Eur J Appl Physiol* 116:1485–1494
- Tous-Fajardo J, Moras G, Rodriguez-Jimenez S, Usach R, Doutres DM, Maffiuletti NA (2010) Inter-rater reliability of muscle contractile property measurements using non-invasive tensiomyography. *J Electromyogr Kinesiol* 20:761–766
- Vierck J, O'Reilly B, Hossner K, Antonio J, Byrne K, Bucci L, Dodson M (2000) Satellite cell regulation following myotrauma caused by resistance exercise. *Cell Biol Int* 24:263–272
- Vigotsky AD, Contreras B, Beardsley C (2015) Biomechanical implications of skeletal muscle hypertrophy and atrophy: a musculo-skeletal model. *PeerJ* 3:e1462
- Wheeler AA, Jacobson BH (2013) Effect of whole-body vibration on delayed onset muscular soreness, flexibility, and power. *J Strength Cond Res* 27:2527–2532
- Wiewelhove T, Raeder C, Meyer T, Kellmann M, Pfeiffer M, Ferrauti A (2016) Effect of repeated active recovery during a high-intensity interval training shock microcycle on markers of fatigue. *Int J Sports Physiol Perform*. doi:10.1123/ijsp.2015-0494
- Zhou S (2000) Chronic neural adaptations to unilateral exercise: mechanisms of cross education. *Exerc Sport Sci Rev* 28:177–184